Journal of Theoretical Biology 255 (2008) 269–277

Contents lists available at ScienceDirect

Journal of Theoretical Biology

journal homepage: www.elsevier.com/locate/yjtbi

The transition from differential equations to Boolean networks: A case study in simplifying a regulatory network model

Maria Davidich *, Stefan Bornholdt

Institute for Theoretical Physics, University of Bremen, Otto-Hahn-Allee, D-28359 Bremen, Germany

ARTICLE INFO

Article history:
Received 8 May 2008
Received in revised form
10 July 2008
Accepted 11 July 2008
Available online 23 July 2008

Keywords:
Gene regulatory networks
Boolean networks
Computer simulations
Differential equations
Fission yeast
Cell cycle

ABSTRACT

Methods for modeling cellular regulatory networks as diverse as differential equations and Boolean networks co-exist, however, without much closer correspondence to each other. With the example system of the fission yeast cell cycle control network, we here discuss these two approaches with respect to each other. We find that a Boolean network model can be formulated as a specific coarse-grained limit of the more detailed differential equations model for this system. This demonstrates the mathematical foundation on which Boolean networks can be applied to biological regulatory networks in a controlled way.

1. Introduction

A major task of molecular cell biology is to comprehend the control of cellular processes of living cells encoded in the genome of the cell. These cellular processes are guided by sophisticated networks of interactions between the macromolecules of the cell as proteins, nucleic acids, and polysaccharides. Their structures and complexes define the unique interactions that control the functions of the cell such as, for example, catalysis of chemical transformations, production of movement, and heredity. The complexity of these processes demands not only advanced experimental techniques, but also adequate mathematical and computational models for understanding them (Gunsalus et al., 2005; Riel, 2006).

Today, there are different methods for modeling the complex networks of biochemical interactions, ranging from master equations based on first principles and the Monte-Carlo method (Gillespie, 1976, 1977), ordinary differential equations (ODE) (Aguda, 2006; Chen et al., 2000; Novak and Tyson, 1993, 1997, 2004; Novak et al., 2001; Sveiczer et al., 2000; Tyson et al., 2001, 2003), stochastic differential equations (Fokker–Plank equations), all the way to Boolean networks (Albert and Othmer, 2003; Bornholdt, 2005; Sanchez et al., 1997; Sanchez and Thieffry, 2001; Thomas et al., 1995).

Among these methods, a most popular approach to modeling biochemical networks is via differential equations, based on the known chemical kinetics, which is successfully applied to describing numerous processes in living organisms (Chen et al., 2000; Novak and Tyson, 1993, 1997, 2004; Novak et al., 2001; Tyson et al., 2002). To build an ODE model, one starts with a schematic diagram representing the known interactions between components. Then this diagram is converted into a set of differential and algebraic equations. The full ODE model then consists of this set of rate equations, plus a set of parameter values and a set of initial conditions. The solutions of the ODEs give the time-dependence of each component of the system. In practice, these solutions depend on rather detailed knowledge about all reactions and kinetic parameters.

In studies where prediction of exact reaction times is not of central interest, simpler models than ODE models and fewer parameters may be sufficient for predicting the course of events in a regulatory network. For example, relevant features of cell commitment, cell cycle progression, and cell differentiation are already described in terms of a sequence of regulatory events (Albert and Othmer, 2003; Braunewell and Bornholdt, 2006; Davidich and Bornholdt, 2008; Li et al., 2004; Sanchez and Thieffry, 2001). In such cases, the much simpler modeling framework of Boolean networks may be a suitable method (Kauffman, 1969; Thomas, 1973). Constructing a Boolean network model starts from a wiring diagram of interactions between

* Corresponding author: Tel.: +49 421 218 3195; fax: +49 421 218 9104.
E-mail addresses: davidich@itp.uni-bremen.de (M. Davidich), bornholdt@itp.uni-bremen.de (S. Bornholdt).

0022-5193/$ - see front matter © 2008 Published by Elsevier Ltd.
doi:10.1016/j.jtbi.2008.07.020

biochemical elements as well, but no kinetic details are needed. Interactions are classified into just two classes, activation or inhibition, as well as the concentration levels being reduced to just an ON or OFF state.

Despite their extreme simplicity, such Boolean models are able to reproduce regulatory sequences, for example, models of genetic networks of *A. thaliana* (Espinosa-Soto et al., 2004; Mendoza et al., 1999; Thum et al., 2003), the cell cycle network of *S. cerevisiae* (Li et al., 2004), the mammalian cell cycle (Faure et al., 2006), and the segment polarity gene network in *D. melanogaster* (Albert and Othmer, 2003; Sanchez and Thieffry, 2001). These examples show that the Boolean network approach provides reliable results for different organisms.

The two diverse methods summarized above (ODE and Boolean networks) are both based on the same "wiring" diagram of interactions between the components, however, use much different amounts of information about these interactions. This poses the interesting question how these two methods are related to each other. A first correspondence between Boolean networks and ODEs has been drawn by Glass and Kauffman (1973) and Glass and Hill (1998) who explored the relationship between a class of non-linear equations representing biochemical control networks and homologous switching networks. They argued that such a correspondence can be achieved with the following requirements: (1) Rates of reactions are described by monotonic sigmoidal functions having distinct upper and lower asymptotes. (2) The parameters must be defined to match the upper or lower asymptote. (3) The target control function must correspond to the maximal or basal rate of biochemical processes. They subsequently demonstrated that there is a large variety of such functions as, e.g. the Heaviside function, the error function, or the Hill function defined for positive arguments.

This leads to a mapping between asymptotical solutions of the ODE system and the Boolean system, while omitting the exact way of transitions between dynamical states.

In this paper, we further explore the correspondence between ODE and Boolean network models considering a specific biological system and demonstrate how a working Boolean model can be derived in terms of a mathematically well defined coarse-grained limit of an underlying ODE model. As our working example we choose the fission yeast cell cycle control network (*Schizosaccharomyces pombe*). The division cell cycle consists of four phases G1–S–G2–M, during which DNA is replicated and the cell divides itself into two cells. The main role is played by "cyclin–dependent–kinases" (CDKs) and cyclins that bind to CDKs to form complexes. CDKs, while being present at all times, can only be active in complexes with cyclins. Cyclins are synthesized or degraded depending on other regulatory activities. Another important participant of the process is an enzyme complex called the "anaphase-promoting complex" (APC), which targets cyclins for degradation. In summary, "to understand the molecular control of cell reproduction is to understand the regulation of CDK and APC activities" (Tyson et al., 2002). These processes, while being complicated, have been well studied for fission yeast *S. pombe* and successful ODE models exist. We choose the most widespread version of the model (Novak et al., 2001) which will serve us as the starting point of our study.

The article is organized as follows. In Section 2 we show the passage from the ODE system of algebraic differential equations for the fission yeast cell cycle, to the limit of the corresponding Boolean model which we construct. Here, also the difficulties that one may encounter when working with Boolean approaches are discussed. Section 3 explores the dynamics of the derived Boolean model of the fission yeast cell cycle. Finally, in the discussion section, the properties of the obtained system are recapitulated and the Boolean and ODE approaches are compared.

2. Boolean variables and stationary states

The passage from a differential equations model to a Boolean network model requires the mapping of continuous solutions (Novak et al., 2001) into the ON/OFF states of a Boolean network's nodes. In order to achieve this, the time evolution of a function, determined by the rate functions and kinetic constants, has to be replaced with a discrete mapping of the node set into itself. Moreover, the rules of this self-mapping have to be governed by logical functions, connecting the binary states of interacting nodes. The dynamics of the resulting Boolean network is an ordered sequence of states of the network nodes, instead of the continuous time output of the ODE model. Having this in mind, let us find the conditions, which allow to perform the transition from a differential equations model to a Boolean model. In the following, we will first describe the passage from continuous variables to discrete states and, in a second step, construct the logical functions representing the dynamics.

2.1. Stationary states of the ODE system

The model of the fission yeast cell cycle (Novak et al., 2001) is based on the antagonist interaction of the *CDK*-cyclin complex with *APC* (via proteins *Ste*9 and *Slp*1) and *CDK* inhibitor *Rum*1. The CDK-cyclin complex (Cdc2/Cdc13) is represented by two variables—*preMPF* and *MPF* ("maturation promoting factor"). Furthermore, helper molecules (start kinase *SK*, transcription factor *TF*, kinase k_{wee}, phosphatase k_{25}, and time-delay enzyme *IE*) participate in the process. Regulatory interactions between these macromolecules are described by two types of equations—differential equations for $Ste9, Slp1, IEP, M, SK, Rum1, preMPF$ and algebraic equations for k_{wee}, k_{25}, TF, and *MPF* variables. Among the first ones, some are of Michaelis–Menten type ($Ste9, Slp1, IEP$) and some are exponential growth (M, SK) equations. The mass variable M plays a special role as it parametrizes the time evolution in the system. The ODE model (Novak et al., 2001) uses arbitrary units for concentrations in all equations, since there are few data of actual protein concentrations. The kinetic constants determine the right timing of the processes. Solutions of the system show that the concentrations of the major proteins in general rise or decrease steeply.

To make the transition to a Boolean system, we first need to rescale the differential equations such that their solutions assume values between 0 (inactive) and 1 (maximum activity). This is a first step towards mapping these variables onto Boolean ON/OFF variables with values 1 and 0. The rescaling does not change the form of equations, it only affects the values of kinetic constants. To do this, let us divide all functions by their respective maximum value. For example, for *Slp*1 we introduce the new rescaled function $Slp1_1 = Slp1\ Ampl$, where $Ampl = 2.1$ is the amplitude of the original solution. Rescaling all variables except M we obtain

$$\frac{\mathrm{d}[Cdc13_{T1}]}{\mathrm{d}t} = k_1 M_1 - (k_2' + k_2''[Ste9_1] + k_2'''[Slp1_1])[Cdc13_{T1}], \tag{1}$$

$$\begin{aligned}\frac{\mathrm{d}[preMPF_1]}{\mathrm{d}t} = {} & k_{wee_1} k_0 (k_0''[Cdc13_{T1}] - [preMPF_1]) \\ & - k_{25} k_0'''[preMPF_1] - (k_2' + k_2''[Ste9_1] \\ & + k_2'''[Slp1_1])[preMPF_1],\end{aligned} \tag{2}$$

$$\begin{aligned}\frac{\mathrm{d}[Ste9_1]}{\mathrm{d}t} = {} & (k_3' + k_3''[Slp1_1]) \frac{1 - [Ste9_1]}{J_3 + 1 - [Ste9_1]} - (k_4'[SK_1] \\ & + k_4[MPF_1]) \frac{[Ste9_1]}{J_4 + [Ste9_1]},\end{aligned} \tag{3}$$

$$\frac{[Slp1_{T1}]}{dt} = k'_5 + k''_5 \frac{[MPF_1]^4}{J_5^4 + [MPF_1]^4} - k_6[Slp1_{T1}], \quad (4)$$

$$\frac{[Slp1_1]}{dt} = k_7[IEP_1]\frac{[Slp1_{T1}] - [Slp1_1]}{J_7 + [Slp1_{T1}] - [Slp1_1]} - k_8\frac{[Slp1_1]}{J_8 + [Slp1_1]} - k_6[Slp1_1], \quad (5)$$

$$\frac{d[IEP_1]}{dt} = k_9[MPF_1]\frac{1 - k'_9[IEP_1]}{J_9 + 1 - k'_9[IEP_1]} - k_{10}\frac{k'_9[IEP_1]}{J_{10} + k'_9[IEP_1]}, \quad (6)$$

$$\frac{d[Rum1_{T1}]}{dt} = k_{11} - (k_{12} - k'_{12}[SK_1] + k''_{12}[MPF_1])[Rum1_{T1}], \quad (7)$$

$$\frac{d[SK_1]}{dt} = k_{13}[TF_1] - k_{14}[SK_1], \quad (8)$$

$$\frac{dM}{dt} = \mu M, \quad (9)$$

$$[TF_1] = G(k_{15}M, k'_{16} + k''_{16}[MPF_1], J_{15}, J_{16}), \quad (10)$$

$$k_{wee_1} = k'_{wee} + (k''_{wee} - k'_{wee})G(V_{awee}, V_{iwee}[MPF_1], J_{awee}, J_{iwee}), \quad (11)$$

$$k_{25_1} = k'_{25} + (k''_{25} - k'_{25})G(V_{a25}[MPF_1], V_{i25}, J_{a25}, J_{i25}), \quad (12)$$

$$[MPF_1] = \frac{(k_{17}[Cdc13_{T1}] - k'_{17}[preMPF_1])([k_{17}[Cdc13_{T1}] - k''_{17}[Trimer])}{k'''_{17}[Cdc13_{T1}]}, \quad (13)$$

$$Trimer = \frac{k_{18}[Cdc13_{T1}][Rum1_{T1}]}{\sigma + \sqrt{\sigma^2 - k'_{18}[Cdc13_{T1}][Rum1_{T1}]}}, \quad (14)$$

$$\sigma = k'_{19}[Cdc13_{T1}] + k''_{19}[Rum1_{T1}] + K_{diss}, \quad (15)$$

where the Goldbeter–Koshland (GK) (Goldbeter and Koshland, 1981; Novak et al., 2001) function has the following general form:

$$G(a,b,c,d) = \frac{2ad}{b - a + bc + ad + \sqrt{(b - a + bc + ad)^2 - 4ad(b - a)}}. \quad (16)$$

Square brackets denote the concentrations of their elements. The subscript 1 marks the rescaled variables with maximum 1. The new values of parameters are shown in Table 1.

Next we map the continuous solution of the ODE model (Novak et al., 2001) into the discrete states of a Boolean network's nodes. Since in a Boolean network model there is no continuous time, but rather a sequence of switching events between states of the nodes, the easiest way to map the continuous solution of ODEs onto the discrete states of a Boolean network's nodes is to reduce (wherever possible) the dynamics of the ODE system to a sequence of stationary states. With stationary states we denote phases in which concentrations do not vary much over time. An observation that helps in this respect is that in most cases the functions of protein concentrations have steep shapes. This means that the system then jumps between two states with a relative short time of transition between them, which one can interpret as an evolution through a number of stationary states.

Table 1
Parameter values for the rescaled system of differential equations

$Cdc13_{T1}$	$k_1 = 0.04, k'_2 = 0.03, k''_2 = 1, k'''_2 = 0.21$
$preMPF_1$	$k'_0 = 1.5, k''_0 = 1.17, k'''_0 = 5$
$Ste9_1$	$k'_3 = 1, k''_3 = 21, J_3 = 0.01, k'_4 = 1.98, k_4 = 50.75$
$Slp1_{T1}$	$k'_5 = 0.002, k''_5 = 0.143, k'_6 = 0.048, J_5 = 0.20689$
$Slp1_1$	$k_7 = 0.429, k_8 = 0.119, J_7 = 0.0005, J_8 = 0.0005$
IEP_1	$k_9 = 0.16, J_9 = 0.01, k_{10} = 0.01, J_{10} = 0.011\ k'_9 = 0.91$
$Rum1_1$	$k_{11} = 0.698, k_{12} = 0.01, k'_{12} = 0.99, k''_{12} = 4.35$
SK_1	$k_{13} = 0.1, k_{14} = 0.1$
M	$\mu = 0.005$
TF_1	$k_{15} = 3, k_{16} = 1, k'_{16} = 2.9, J_{15} = 0.01, J_{16} = 0.01$
k_{wee_1}	$k'_{wee} = 0.115, k''_{wee} = 1, V_{iwee} = 1.45, V_{awee} = 0.25, J_{awee} = 0.01, J_{iwee} = 0.01$
k_{25_1}	$k'_{25} = 0.01, k''_{25} = 1, V_{i25} = 0.25, V_{awee} = 0.36, J_{a25} = 0.01, J_{iwee} = 0.01, J_{i25} = 0.01$
MPF	$k'''_{17} = 0.69, k_{17} = 1.5, k'_{17} = 1.3, k''_{17} = 1.5, k'''17 = 1.5$
Trimer	$k_{18} = 0.441, k'_{18} = 0.882$
σ	$k'_{19} = 1.5, k''_{19} = 0.147, K_{diss} = 0.001$

The evolution through the cell cycle as a sequence of stationary states was modeled by Novak et al. (2001), who represented the cell cycle dynamics using bifurcation diagrams. The main idea of bifurcation analysis is that there exist some parameters, whose values determine various qualitative behavior of a solution (e.g. stationary asymptotics). Novak et al. (2001) have chosen mass as a main bifurcation parameter, since it plays a role of time. Also other variables can play a role of bifurcation parameters as well with corresponding critical values at the transitions points. Thus, the dynamical evolution of a cell cycle could be reduced to the sequence of critical values of bifurcation parameters determining the various kinds of the systems' stationary solutions. For our purpose let us use the results of the bifurcation analysis (Novak et al., 2001) of the transitions during the cell cycle.

First, there are some variables ($Ste9, Slp1, IEP$) that are described by GK functions (Novak et al., 2001) in the stationary state:

$$[Ste9_1] = G(k'_3 + k''_3[Slp1_1], k'_4[SK_1] + k_4[MPF_1], J_3, J_4), \quad (17)$$

$$[IEP_1] = 1/k'_9 G(k_9[MPF_1], k_{10}, J_9, J_{10}), \quad (18)$$

$$[Slp1_1] = [Slp1_{T1}]G(k_7[IEP_1], k_8, J_7/[Slp1_{T1}], J_8/[Slp1_{T1}]). \quad (19)$$

The characteristic properties of the GK function imply that its variable mainly resides in two limiting states: high and low. The transition region between them is short (as the variables J are small). Therefore, we approximate them as Boolean (binary) variables.

It is easy to see that $Slp1_{T1}$ determines only the amplitude and the smoothness of the transition in (19), therefore, we neglect $Slp1_{T1}$ as a first step towards a Boolean model and write

$$[Slp1_1] = G(k_7 IEP_1, k_8, J, J). \quad (20)$$

The states of the remaining variables can be described by GK functions, as well. For SK, while the equation for this variable is exponential, one can evaluate the right-hand part through a GK function with the stationary solution (Novak et al., 2001):

$$[SK_1] = (k_{13}/k_{14})[TF] = (k_{13}/k_{14})G(k_{15}M_1, k'_{16} + k''_{16}[MPF_1], J_{15}, J_{16}). \quad (21)$$

Furthermore, there are three algebraic equations for TF (10), k_{wee} (11), and k_{25} (12) that contain GK functions. Here, again, the two limiting states of the GK function will be related to the binary ON/OFF states of the corresponding variables in the Boolean limit.

Finally, we will simplify the functional behavior for the $Cdc13_T, preMPF$, and $Rum1_T$, as well. Again we want to neglect the exact path of their transitions, keeping the limiting stationary states, eventually enabling us to take the limit of Boolean functions as a simplified description of the dynamics. Equations with the following requirements will allow us to take this limit:

(a) In a small neighborhood of the switching point, the functional behavior can be approximated by an exponential rise.
(b) On the larger interval, it has a stationary solution with a steep transition between two limiting stationary states.

(c) This function converges to the Heaviside function in the limit of steep transition.

In the following we will see that the Michaelis–Menten dynamics fulfills these requirements, resulting in exact conformity of initial and final states and permitting a well controlled passage to a Boolean function. Here and below we refer to this kind of equations as Michaelis–Menten for simplicity, in spite of the fact that they actually combine two Michaelis–Menten terms corresponding to two opposing processes:

$$\frac{dX}{dt} = k_1 \frac{1-X}{J_1+1-X} - k_2 \frac{X}{J_2+X}. \tag{22}$$

Let us first check condition (a). Expanding (22) in the neighborhood of switching points where $X \ll J_{1,2} \ll 1$ and keeping leading order terms yields

$$\frac{dX}{dt} = k_1 - \frac{k_2}{J_2} X. \tag{23}$$

This is a common equation of exponential growth/decrease. It allows us to take equations of exponential growth as an expansion of (23) in the neighborhood of switching ON/OFF points. For $Cdc13_T$, for example, the equation

$$\frac{d[Cdc13_{T1}]}{dt} = k_1 M - (k_2' + k_2''[Ste9_1] + k_2'''[Slp1_1])[Cdc13_{T1}] \tag{24}$$

is the expansion of the equation

$$\frac{d[Cdc13_{T1}]}{dt} = k_1 M \frac{1-[Cdc13_{T1}]}{J_1+1-[Cdc13_{T1}]} - (k_2' + k_2''[Ste9_1] + k_2'''[Slp1_1])[Cdc13_{T1}] \frac{[Cdc13_{T1}]}{J_2+[Cdc13_{T1}]}. \tag{25}$$

For illustration, in Fig. 1, this function is compared with the initial $Cdc13_{T1}$.

Condition (b) is satisfied as well, since the stationary states of (22) are described by a GK function. Validity of condition (c) will be shown in the next section.

Thus, for the above equations we have a system of GK functions which are responsible for the transitions between stationary states:

$$[Cdc13_{T1}] = G(k_1 M, k_2''[Ste9_1] + k_2'''[Slp1_1], J, J), \tag{26}$$

$$[preMPF_1] = G(k_0 k_{wee}[Cdc13_{T1}], [k_{wee_1}] + k_0''[k_{25_1}] + k_2' + k_2''[Ste9_1] + k_2'''[Slp1_1], J, J), \tag{27}$$

$$[Rum1_{T1}] = G(k_{11}, k_{12} + k_{12}'[SK_1] + k_{12}''[MPF_1], J, J). \tag{28}$$

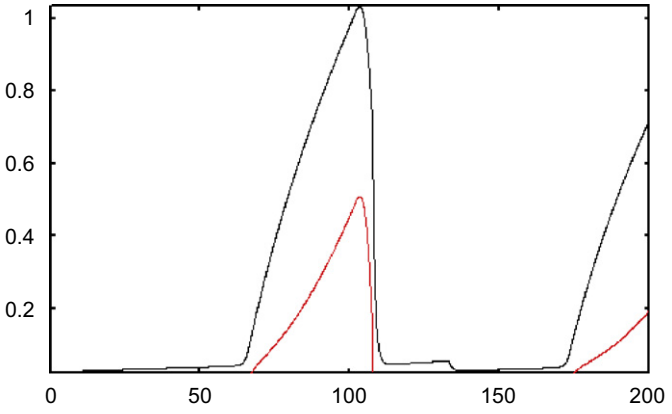

Fig. 1. Numerical simulation of (24) (black curve) and (25) (red (gray) curve). Note that the downward decrease occurs practically simultaneously.

One can see in Fig. 1 that the new and initial functions start to grow and start to decrease at the same times, respectively. Note that the obtained substituted equations (26)–(28) play only a helper role and cannot be directly applied to the initial system of differential equations. The complete correspondence of the obtained system to the initial one is achieved by the limit transition shown in Section 2.2.

Summarizing all information above we obtain the system of equations (10)–(12), (17) and (18), (20) and (21), (26)–(28), describing the stationary states of the corresponding variables. The next step is to perform a transition from the continuous functions to discrete functions.

2.2. Transition to Boolean variables

We here show that there is an exact passage from the function of Goldbeter and Koshland (1981) to the indicator function (Heaviside step function). Let us remark that in (16) the parameters a and b are functional variables, whereas c and d (in (10)–(12), (17) and (18), (20) and (21), (26)–(28), they are denoted as variables J) are usually fixed and small in all equations. The range of values of c, d varies from 0.001 to 0.01 and only one time for $Slp1$ it takes on the value 0.3. Very small parameters c and d mean that the enzyme-substrate complex is tightly bound and hardly dissociates. Thereby in Novak et al. (2001) an assumption is made that the enzyme-substrate complexes involved are very stable (Aguda, 2006). For this reason, let us consider the behavior of the corresponding GK functions in the limiting case $c \to 0, d \to 0$ while a and b take finite values.

First note that, both, numerator and denominator depend on d. Moreover, a is a numerator's factor. At the same time, c appears in a sum with the finite terms in the denominator, only (except at the point $b = a$). Therefore, we can assume, without loss of generality, that $c = 0$ and consider below

$$G(a,b,0,d) = \frac{2ad}{b-a+ad+\sqrt{(b-a+ad)^2-4ad(b-a)}}.$$

Using the Taylor expansion of the square root in the denominator and neglecting higher powers of d, we obtain for all points $a \neq b$

$$G(a,b,0,d) = \frac{2ad}{b-a+ad+|b-a|-ad\frac{b-a}{|b-a|}}. \tag{29}$$

There are two possible cases:

- if $b-a>0$ then $|b-a| = b-a$ and (29) takes a form
  $$G(a,b,0,d) = \frac{2ad}{b-a};$$
- if $b-a<0$ then $|b-a| = -(b-a)$ and (29) is simply $G(a,b,0,d) = 1$.

This implies that, in this limit, there is a transition from the GK function $G(a,b,c,d)$ to the Heaviside function $\theta(a-b)$:

$$\lim_{c,d\to 0} = \theta(a-b) = \begin{cases} 0, & a<b, \\ 1, & a>b. \end{cases}$$

Thus, in this limit, the variable a plays the role of an activator input and the variable b is an inhibitor input. The output is active/inactive (its Boolean value is equal to one/zero) if the total value of activator inputs is larger/smaller than the total value of inhibitor inputs. Thus, the GK function converges to the Heaviside function in the limit of steep transitions.

2.3. Logical Boolean functions

Let us now rewrite the system of equations in the limit of the parameters $J \to 0$ (i.e., the parameters $J_3, J_5, J_7, J_8, J_{10}, J_{16}, J_{awee}, J_{iwee}, J_{i25}, J_{a25}$ and the corresponding parameters J in Eqs. (20), (26)–(28) equations) as

$$[Ste9_1] = \theta(k'_3 + k''_3[Slp1_1] - k'_4[SK_1] - k_4[MPF_1]), \tag{30}$$

$$[IEP_1] = \theta(k_9[MPF_1] - k_{10}), \tag{31}$$

$$[SK_1] = (k_{13}/k_{14})\theta(k_{15}M_1 - k'_{16} - k''_{16}[MPF_1]), \tag{32}$$

$$[TF_1] = \theta(k_{15}M - k'_{16} - k''_{16}[MPF_1]), \tag{33}$$

$$[k_{wee_1}] = k'_{wee} + (k''_{wee} - k'_{wee})\theta(V_{awee} - V_{iwee}[MPF_1]), \tag{34}$$

$$[k_{25_1}] = k'_{25} + (k''_{25} - k'_{25})\theta(V_{a25}[MPF_1] - V_{i25}), \tag{35}$$

$$[Cdc13_{T1}] = \theta(k_1 M - k''_2[Ste9_1] - k'''_2[Slp1_1]), \tag{36}$$

$$[preMPF_1] = \theta(k_{wee}[Cdc13_{T1}] - [k_{wee_1}] - [k_{25_1}] - k'_2 - k''_2[Ste9_1] - k'''_2[Slp1_1]), \tag{37}$$

$$[Rum1_{T1}] = \theta(k_{11} - k_{12} - k'_{12}[SK_1] - k''_{12}[MPF_1]), \tag{38}$$

$$[Slp1_1] = \theta(k_7[IEP_1] - k_8). \tag{39}$$

Let us add two simplifications to the Eqs. (32), (34) and (35). In Eq. (32), the coefficient $k_{13}/k_{14} = 1$ and thus can be neglected. In Eq. (34), k_{wee_1} can have two possible values: 0.115 and 1. The first one can be reduced to 0 since it does not change the behavior of the system and analogously for k_{25}

$$[k_{wee_1}] = \theta(V_{awee}, V_{iwee}[MPF_1], J_{awee}, J_{iwee}), \tag{40}$$

$$[k_{25_1}] = \theta([MPF_1] - V_{i25}), \tag{41}$$

$$[SK_1] = \theta(k_{15}M - k'_{16} - k''_{16}[MPF_1]). \tag{42}$$

As a result we have a system of 10 equations, where all variables, except *MPF* and *M* take values 0 or 1. *MPF* and *M* cannot be described in this formalism. *MPF* is represented by an algebraic equation which cannot be reduced to the GK function. Taking a closer look, the solution of *MPF* does not reach a simple stationary state, instead there are three typical states of *MPF* in the system (*preMPF*, *Rum*1, *Cdc*13)—OFF, intermediate and high activation.

(1) If $Cdc13 = 0$ then $MPF = 0$, independently of the states of *preMPF* and *Rum*1.
(2) If $Cdc13 = 1$ and $preMPF = 1$ then $MPF = 0.14$, independently of the state of *Rum*1. This corresponds to an intermediate level, where *preMPF* prevents high excitation.
(3) If $Cdc13 = 1, preMPF = 0$, and $Rum1 = 1$, then $MPF = 1$, with its value slightly decreasing to $MPF = 0.93$ if $Rum1 = 0$. This corresponds to a high level of activation, when *MPF* is activated by *Cdc*13 and this activation is not reduced by *preMPF*.

Let us reformulate these rules in the following. Assume there are two variables—*MPF* and *MPF*2. The first one is activated by *Cdc*13. For activation of the second variable *MPF*2, one assumes that *MPF* has to be present at a low level and *preMPF* should be inactive. Thereby, one needs to rewrite the system of Eqs. (30), (36) and (37) taking into account which level of excitation of *MPF* is crucial for each particular variable.

$$[MPF_1] = \theta(Cdc13_{T1}), \tag{43}$$

$$[MPF2] = \theta(MPF_1 - [preMPF_1]), \tag{44}$$

$$[IEP_1] = \theta([k_9[MPF_1] - k_{10}), \tag{45}$$

$$[TF_1] = \theta(k_{15}M - k'_{16} - k''_{16}[MPF2_1]), \tag{46}$$

$$[Rum1_{T1}] = \theta(k_{11} - k_{12} - k'_{12}[SK_1] - k''_{12}[MPF_1]), \tag{47}$$

$$[k_{wee_1}] = \theta(V_{awee} - V_{iwee}[MPF_1]), \tag{48}$$

$$[k_{25_1}] = \theta([MPF_1] - V_{i25}), \tag{49}$$

$$[SK_1] = \theta([TF]), \tag{50}$$

$$[Ste9_1] = \theta(k'_3 + k''_3[Slp1_1] - k'_4[SK_1] - k_4([MPF_1])). \tag{51}$$

Second, as in the model based on differential equations the cell mass *M* takes a special role in the present model. The solution (Novak et al., 2001) treats it during a cell growth as an independent variable, which is described by an exponential growth function (9). Thus, the variable *M* corresponds to a time in this system, which drives the evolution between stationary states (Novak et al., 2001). In the system, *M* directly influences *Cdc*13 and *TF*. As soon as *M* reaches a threshold value, it activates *Cdc*13 and induces the sequence of consecutive transitions between stationary states. For *TF* it plays a role of constantly positive input, *TF* is always active unless *MPF* has a high activity.

As a criterium for the end of the cycle, Novak et al. (2001) determine when the cell divides by monitoring the values of the other variables. When these chosen variables have certain values that indicate the end of the cell cycle, the current value of *M* is divided by two manually, as at the end of mitosis the cell divides into two daughter cells of approximately equal masses. Subsequently, *M* continues its exponential growth, again.

Following this strategy, one needs to distinguish *M* between two principal different values—*M* and 2*M* in the Boolean model. Here *M* works at the beginning of the cell cycle as a trigger of switching events, whereas 2*M* plays a role of an indicator for the end of the cell cycle. Correspondingly, *M* becomes 2*M* at the end of mitosis, when *Slp*1, *Ste*9, and *IEP* all have high concentrations.

Therefore, one can add the following Boolean rules:

$$M = \theta(2M - [Ste9_1][Slp1_1][IEP_1]), \tag{52}$$

$$2M = \theta(M[Ste9_1][Slp1_1][IEP_1] - 2M). \tag{53}$$

Thus, we have a system of equations (43)–(53), where each variable can take values 0 or 1, only. It is easy to simplify this system, reducing the kinetic coefficients to 0 or 1 and adding thresholds. Consider, for example, $Cdc13_T$. In Table 2, based on Eq. (36), we show all possible cases for *Cdc*13. In a more compact form, where the kinetic constants are reduced to 1, these rules become

$$[Cdc13_{T1}] = \theta(M - [Ste9_1] - [Slp1_1]). \tag{54}$$

Table 2
Boolean rules for variable *Cdc*13

Number	*M*	*Ste*9	*Slp*1	*Cdc*13
1	0	0	0	0
2	1	0	0	1
3	1	1	0	0
4	1	1	1	0
5	0	1	0	0
6	0	1	1	0
7	1	0	1	0
8	1	1	1	0

Repeating the same procedure for all variables, we obtain the system of equations:

$$[preMPF_1] = \theta(k_{wee} + [Cdc13_{T1}] - 1 - [k_{25_1}] - [Ste9_1] - [Slp1_1]), \tag{55}$$

$$[Slp1_1] = \theta([IEP_1]), \tag{56}$$

$$[TF_1] = \theta([M] + [2M] - [MPF2_1]), \tag{57}$$

$$[IEP_1] = \theta([MPF_2]), \tag{58}$$

$$[Rum1_{T1}] = \theta(0.5 - [SK_1] - [MPF_1]), \tag{59}$$

$$[k_{wee_1}] = \theta(0.5 - [MPF_1]), \tag{60}$$

$$[k_{25_1}] = \theta([MPF_1] - 0.5), \tag{61}$$

$$[SK_1] = \theta([TF_1]), \tag{62}$$

$$[Ste9_1] = \theta([Slp1_1] - [SK_1] - [MPF_1]), \tag{63}$$

$$M = \theta(2M + 3 - [Ste9_1] - [Slp1_1] - [IEP_1]), \tag{64}$$

$$2M = \theta(M + [Ste9_1] + [Slp1_1] + [IEP_1] - 3 - 2M). \tag{65}$$

3. Boolean model

We now have a system of algebraic equations (54)–(63), which describe the switch-like transitions between stationary states, plus Boolean equations (43) and (44), (64) and (65) for M and MPF. Note that in this discrete system, no information about continuous time is present any more, except the sequence of events. To obtain this discrete dynamical sequence, we iteratively solve the system. We start from the known initial conditions (Novak et al., 2001): $2M = 1, Slp1_1 = 1, IEP_1 = 1, Ste9_1 = 1$, $k_{wee1} = 1$, with all other variables being 0. Following the terminology of Boolean models, each variable is represented by one node. The network of nodes is shown in Fig. 2. Each node i has only two states, $S_i(n) = 1$ (active) and $S_i(n) = 0$ (inactive). The index n is the number of iterations. The iterative solution of the system has the following general form:

$$S_i(n+1) = \theta\left(\sum_k T_{ik} S_k(t) + Q_i\right), \tag{66}$$

with the Heaviside function

$$\theta(x) = \begin{cases} 1, & x > 0 \\ 0, & x \leqslant 0. \end{cases} \tag{67}$$

All nodes are updated synchronously, which corresponds to the iteration of the full dynamical system. The interaction matrix T_{ik} and the state vector Q_i determine the transition rule between states.

The specific values of the interactions T_{ik} are determined as follows. All interactions between a pair of nodes are defined by an interaction strength given as the elements T_{ik} and an activation threshold Q_i. Positive (negative) arguments of the θ-functions have $T_{ik} = 1$ ($T_{ik} = -1$). $T_{ii} = 1$ for M, this rule is true only for M node, since it is described by a growing exponential function.

The resulting matrix T_{ik} and vector Q_i have the following form:

$$T_{ik} = \begin{array}{c} \\ Cdc13T \\ preMPF \\ MPF \\ MPF2 \\ k25 \\ k_{wee} \\ M \\ Slp1 \\ Ste9 \\ TF \\ SK \\ 2M \\ IEP \\ Rum1 \end{array} \begin{array}{c} \begin{array}{cccccccccccccc} Cdc13T & preMPF & MPF & MPF2 & k25 & k_{wee} & M & Slp1 & Ste9 & TF & SK & 2M & IEP & Rum1 \end{array} \\ \begin{pmatrix} 0 & 0 & 0 & 0 & 0 & 0 & 1 & -1 & -1 & 0 & 0 & 0 & 0 & 0 \\ 1 & 0 & 0 & 0 & -1 & 1 & 0 & -1 & -1 & 0 & 0 & 0 & 0 & 0 \\ 1 & 0 & 0 & 0 & 0 & 0 & 0 & 0 & 0 & 0 & 0 & 0 & 0 & 0 \\ 0 & -1 & 1 & 0 & 0 & 0 & 0 & 0 & 0 & 0 & 0 & 0 & 0 & 0 \\ 0 & 0 & 1 & 0 & 0 & 0 & 0 & 0 & 0 & 0 & 0 & 0 & 0 & 0 \\ 0 & 0 & -1 & 0 & 0 & 0 & 0 & 0 & 0 & 0 & 0 & 0 & 0 & 0 \\ 0 & 0 & 0 & 0 & 0 & 0 & 1 & -1 & -1 & 0 & 0 & 1 & -1 & 0 \\ 0 & 0 & 0 & 0 & 0 & 0 & 0 & 0 & 0 & 0 & 0 & 0 & 1 & 0 \\ 0 & 0 & -1 & 0 & 0 & 0 & 0 & 1 & 0 & 0 & -1 & 0 & 0 & 0 \\ 0 & 0 & 0 & -1 & 0 & 0 & 1 & 0 & 0 & 0 & 0 & 1 & 0 & 0 \\ 0 & 0 & 0 & 0 & 0 & 0 & 0 & 0 & 0 & 1 & 0 & 0 & 0 & 0 \\ 0 & 0 & 0 & 0 & 0 & 0 & 0 & 1 & 1 & 0 & 0 & -1 & 1 & 0 \\ 0 & 0 & 0 & 1 & 0 & 0 & 0 & 0 & 0 & 0 & 0 & 0 & 0 & 0 \\ 0 & 0 & -1 & 0 & 0 & 0 & 0 & 0 & 0 & 0 & -1 & 0 & 0 & 0 \end{pmatrix} \end{array}, \tag{68}$$

$$Q_i^{\mathrm{T}} = (0 \;\; -1 \;\; 0 \;\; 0 \;\; -0.5 \;\; 0.5 \;\; 3 \;\; 0 \;\; 0 \;\; 0 \;\; 0 \;\; -3 \;\; 0 \;\; 0.5). \tag{69}$$

4. Results of Boolean simulation of the fission yeast cell cycle

First we run the model described in the previous section with the initial conditions (Novak et al., 2001). The temporal evolution of the protein states is presented in Table 3. One can see that the iterative solution of system (43) and (44), (54)–(65) is the switching between unstable stationary states, which coincide with the corresponding evolution in the ODE model. The final state is a stable stationary state of the system. One notices that the initial and end states are identical except for the activation of the nodes M and $2M$. The update of nodes M and $2M$, keeping all other nodes in the same states, starts the new cycle. This cycling of the model is similar to the realization of cycling in the original model of differential equations.

Let us briefly summarize our coarse-graining strategy that we followed in this article.

In Fig. 3, we show consecutive abstractions of the model for the $Ste9$ and IEP variables as an example. For this we first plot the dynamics of the differential equations model, then the evolution between the stationary states solutions of the ODE model, and finally the sequence of states obtained from the iterated Boolean network model.

In the next step we run the model starting from each of the 2^{15} possible initial states. We find that from all initial states 67% flows

into one big attractor. This attractor is the same stable stationary state that one obtains starting with biological conditions described above.

4.1. Mutations

Let us also compare the behavior of mutants. We model two mutations—*Wee*$^-$ and *Wee*$^-$*Cdc*25△ described in Novak et al. (2001). In Boolean models one cannot distinguish between reduced activity and no activity. This is why we model *Wee*$^-$ as *Wee*△ in both cases. We run the model starting with wild type initial conditions, but with deleted nodes k_{wee}, and in the second case k_{wee} and k_{25}. In both mutations, the number of steps is reduced to 12, as compared to 14 in the wild type cell cycle described in the previous section. This suggests that the cell can divide at a smaller size than the wild type, where both mutations are viable. Our results are in accordance with the predictions of the earlier differential equation model (Novak et al., 2001).

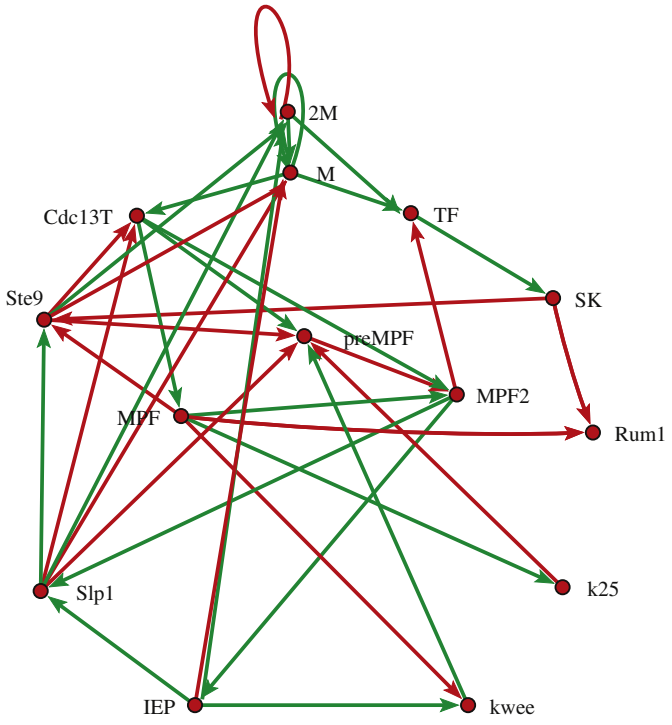

Fig. 2. Interaction network of the Boolean model. Green links correspond to $T_{ik} = +1$ and red links to $T_{ik} = -1$.

4.2. Comparison with an existing Boolean model for the fission yeast cell cycle

It is interesting to compare this model with an earlier Boolean model for the fission yeast cell cycle (Davidich and Bornholdt, 2008) that was built on known biochemical interactions between proteins, only. Both models are quite similar and have the same connections between homologue nodes. Their dynamics matches the wild type signaling sequence during the cell cycle. The difference is that in the current model the nodes *Cdc*13, *preMPF*, *MPF*1, *MPF*2 correspond to only two nodes Cdc2/Cdc13 and Cdc2/Cdc13* in Davidich and Bornholdt (2008). Therefore, in the model (Davidich and Bornholdt, 2008), the complex Cdc2/Cdc13 can have two levels of activation—medium and high. The intermediate level corresponds to sole activation of the Cdc2/Cdc13 node, whereas a high level of activation is represented by activation of both, Cdc2/Cdc13 and Cdc2/Cdc13*. The last one plays the role of a dephosphorylated Cdc2/Cdc13, that closely corresponds to *MPF* in Novak et al. (2001). In the current model, the node *MPF* was separated into two nodes *MPF*1 and *MPF*2 as well, to distinguish different levels of *MPF* activation.

The formulas responsible for evolution of proteins are similar in a sense that in both a threshold activation rule is used. In the model (Davidich and Bornholdt, 2008), proteins remain active if the corresponding node was not switched-off by other incoming inhibiting signals. This rule means that if the protein was activated it requires some other signals to change its state, whereas in the current model one needs to have always a positive incoming signal in order to keep the protein in its active form.

5. Discussion and conclusion

In this paper, our aim is to make a connection between two successfully used methods—the ODE and the Boolean network models for predicting properties of a real biological regulatory process. In particular, we show a possible limit transition between the ODE and the Boolean network model for the fission yeast cell cycle control network. For this purpose the known ODE model (Novak et al., 2001) of fission yeast has been chosen.

In order to do the transition, first the differential equations are rewritten in such a way that the solutions of all equations reach 1 in their maximum values. Then the obtained equations are transformed in a limiting procedure to Boolean functions. Firstly, Michaelis–Menten equations and equations with switch-like

Table 3
Temporal evolution of protein states for the cell-cycle control network

Number of iteration	$Cdc13_T$	*preMPF*	*MPF*1	*MPF*2	k_{25}	k_{wee}	*M*	*Slp*1	*Ste*9	*TF*	*SK*	2*M*	*IEP*	*Rum1*
1	0	0	0	0	0	1	0	1	1	0	0	1	1	1
2	0	0	0	0	0	1	1	1	1	1	0	0	0	1
3	0	0	0	0	0	1	1	0	1	0	1	1	0	1
4	0	0	0	0	0	1	1	0	0	1	1	0	0	0
5	1	0	0	0	0	1	1	0	0	1	1	0	0	0
6	1	1	1	0	0	1	1	0	0	1	1	0	0	0
7	1	1	1	0	1	0	1	0	0	1	1	0	0	0
8	1	0	1	0	1	0	1	0	0	1	1	0	0	0
9	1	0	1	1	1	0	1	0	0	1	0	0	0	0
10	1	0	1	1	1	0	1	0	0	0	0	0	1	0
11	1	0	1	1	1	0	1	1	0	0	0	0	1	0
12	0	0	1	1	1	0	1	1	0	0	0	0	1	0
13	0	0	0	1	1	0	1	1	0	0	0	0	1	0
14	0	0	0	0	0	1	1	1	1	0	0	0	1	1

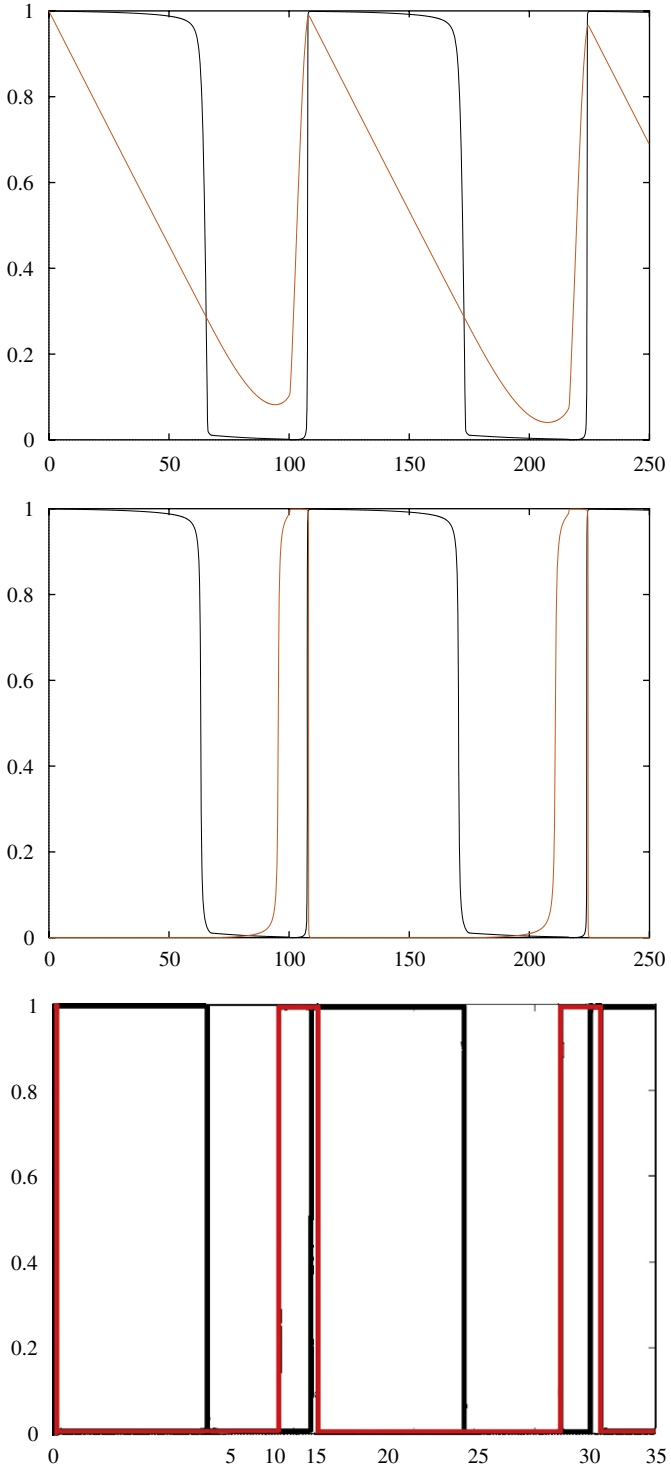

Fig. 3. (a): Dynamics of *IEP* (red (gray) curve) and *Ste*9 (black curve) in the numerical simulation of the system of differential equations. *IEP* (red (gray) curve) and *Ste*9 (black curve). (b) Numerical simulation of stationary states for *IEP* (red (gray) curve) and *Ste*9 (black curve). (c) Boolean networks of dynamical sequence for *IEP* (red (gray) curve) and *Ste*9 (black curve).

behavior can be directly reduced to Boolean functions. Secondly, a set of equations with sigmoidal transfer functions can be replaced with Michaelis–Menten equations without changing the sequence of states through which the system evolves. Thirdly, there are also some cases that cannot be reduced to the two previous ones. It happens when the variable is described by a constantly growing function or a function which has distinctly different levels. In this case, we propose in the Boolean network model to substitute those variables with two, labeling intermediate and high activity of it. Finally, all continuous solutions of the equations are mapped into ON/OFF states of a Boolean network model and the transition between states are described by Boolean functions.

This Boolean model reproduces the results of the initial ODE model (Novak et al., 2001). In particular, starting with initial conditions as in Novak et al. (2001), the system evolves through the same sequence of states. The second evidence of similar behavior of the ODE and the Boolean network model is the robustness w.r.t. changes in the initial conditions. The Boolean model has a dominant attractor (67%), attracting most of the trajectories, starting from different initial conditions. The dominant attractor coincides with the biological initial condition of the system. The ability to model mutations in the Boolean approach additionally confirms a good correspondence between the ODE and the Boolean model.

We find that the transition to a Boolean model is possible for differential equations, which have monotonic sigmoidal functions with distinct upper and lower asymptotes. In particular, firstly, in our case Michaelis–Menten equations are reduced to S-shaped GK functions which have the necessary asymptotes (Glass and Kauffman, 1973; Glass and Hill, 1998). This function works as a switch between the cases when parameters are defined as the upper or lower asymptote and the target control function corresponds to the maximal or basal rate of biochemical processes. Secondly, here substituting some equations that have monotonic sigmoidal functions on the right-hand side with Michaelis–Menten functions, we also find, that the exact form of the sigmoidal function does not strongly influence the behavior of the system. The comparison of the current model with a previous Boolean model for fission yeast reveals that they both have a similar set of variables (proteins) and similar Boolean functions responsible for update.

Our results also confirm the idea that some molecular control networks are so robustly designed that timing is not a critical factor (Braunewell and Bornholdt, 2006). In our case, it is possible to reproduce the main results of Novak et al. (2001) without including time, but reproducing the right sequence of events. It supports the idea that the Boolean approach could contain sufficient information. Thereby one needs less information about the system, the knowledge about reactions on the level of activation/inhibition is sufficient, which eliminates the problem of finding the right kinetic constants. Another advantage is the low computational cost of Boolean networks.

The problems one meets working with the Boolean approach are that it is sometimes difficult to reduce the concentration level of some proteins only to ON/OFF states. Sometimes there are intermediate states of concentration which need to be separated from high concentration. In this case two methods are possible. One is, as we implemented it here, to divide this variable into two and to perform as two different nodes in a system. When doing this, one needs to take into account the differences in interactions of this protein when it has intermediate and high concentration. Another solution for a such situation could be the introduction of two discrete levels of concentration that the protein can have, for example 1 for intermediate and 2 for high concentration, which was used in modeling gene regulatory network model for *Arabidopsis thaliana* flower development (Espinosa-Soto et al., 2004).

We would like to note that the ODE and the Boolean approach are both useful methods. The advantage of the ODE approach is that it provides detailed information about the system at any given time in contrast to the Boolean network method, which reproduces only the right sequence of events. But the costs for this information are considerable. One needs to have exhaustive

information about the reactions, where the most difficult part is to find the right kinetic constants. Also it demands more computational costs to find the solution of the system. One could say that the ODE approach is appropriate when the system is well studied and it is necessary to make a detailed study of all reactions that take place. On the other hand, if the task is to understand the main principles of a regulatory process and one has less information, the Boolean approach may be very suitable to use. It has the potential to extend dynamical modeling to the very early, exploratory phase of inferring the architectural details of a regulatory network. From our study we conclude that Boolean networks can provide a mathematically well founded approach to qualitative modeling of the dynamics of biological regulatory networks.

References

Aguda, D.B., 2006. Modeling the Cell Division Cycle, Lecture Notes in Mathematics, vol. 1872, Springer, Berlin, pp. 1–22.

Albert, R., Othmer, H.G., 2003. The topology of the regulatory interactions predicts the expression pattern of the Drosophila segment polarity genes. J. Theor. Biol. 223, 1–18.

Bornholdt, S., 2005. Systems biology: less is more in modeling large genetic networks. Science 310 (5747), 449–451.

Braunewell, S., Bornholdt, S., 2006. Superstability of the yeast cell-cycle dynamics: ensuring causality in the presence of biochemical stochasticity. J. Theor. Biol. 245 (4), 638–643.

Chen, K.C., Csikasz-Nagy, A., Gyorffy, B., Val, J., Novak, B., Tyson, J.J., 2000. Kinetic analysis of a molecular model of the budding yeast cell cycle. Mol. Biol. Cell 11, 369–391.

Davidich, M., Bornholdt, S., 2008. Boolean network model predicts cell cycle sequence of fission yeast. PLoS ONE 3 (2), e1672.

Espinosa-Soto, C., Padilla-Longoria, P., Alvarez-Buylla, E.R., 2004. A gene regulatory network model for cell-fate determination during *Arabidopsis thaliana* flower development that is robust and recovers experimental gene expression profiles. Plant Cell 16, 2923–2939.

Faure, A., Naldi, A., Chaouiya, C., Thieffry, D., 2006. Dynamical analysis of a generic Boolean model for the control of the mammalian cell cycle. Bioinformatics 22 (14), e124–e131.

Gillespie, D.T., 1976. A general method for numerically simulating the stochastic time evolution of coupled chemical reactions. J. Comp. Phys. 22, 403–434.

Gillespie, D.T., 1977. Exact stochastic simulation of coupled chemical reactions. J. Phys. Chem. 81, 2340–2361.

Glass, L., Hill, C., 1998. Ordered and disordered dynamics in random networks. Europhys. Lett. 41 (6), 599–604.

Glass, L., Kauffman, S.A., 1973. The logical analysis of continuous, nonlinear biochemical control networks. J. Theor. Biol. 39, 103–129.

Goldbeter, A., Koshland, D.E., 1981. An amplified sensitivity arising from covalent modification in biological systems. Proc. Natl. Acad. Sci. USA 78, 6840–6844.

Gunsalus, K.C., Ge, H., Schetter, A.J., Goldberg, D.S., Han, J.-D.J., et al., 2005. Predictive models of molecular machines involved in *Caenorhabditis elegans* early embryogenesis. Nature 436 (11), 861–865.

Kauffman, S.A., 1969. Metabolic stability and epigenesis in randomly constructed genetic nets. J. Theor. Biol. 22, 437–467.

Li, F., Long, T., Lu, Y., Quyang, Q., Tang, C., 2004. The yeast cell-cycle network is robustly designed. Proc. Natl. Acad. Sci. USA 101 (14), 4781–4786.

Mendoza, L., Thieffry, D., Alvarez-Buylla, E.R., 1999. Genetic control of flower morphogenesis in *Arabidopsis thaliana*: a logical analysis. Bioinformatics 15, 593–606.

Novak, B., Tyson, J.J., 1993. Numerical analysis of a comprehensive model of M-phase control in Xenopus oocyte extracts and intact embryos. J. Cell Sci. 106, 1153–1168.

Novak, B., Tyson, J.J., 1997. Modeling the control of DNA replication in fission yeast. Cell biology. Proc. Natl. Acad. Sci. USA 94, 9147–9152.

Novak, B., Tyson, J.J., 2004. A model for restriction point control of the mammalian cell cycle. J. Theor. Biol. 230, 563–579.

Novak, B., Pataki, Z., Ciliberto, A., Tyson, J.J., 2001. Mathematical model of the cell division cycle of fission yeast. Chaos 11 (1), 277–286.

Riel, N.A.W., 2006. Dynamic modelling and analysis of biochemical networks: mechanism-based models and model-based experiments. Briefings Bioinformatics 7 (4), 364–374.

Sanchez, L., Thieffry, D., 2001. A logical analysis of the drosophila gap-gene system. J. Theor. Biol. 211, 115–141.

Sanchez, L., van Helden, J., Thieffry, D., 1997. Establishement of the dorso-ventral pattern during embryonic development of *Drosophila melanogaster*: a logical analysis. J. Theor. Biol. 189 (4), 377–389.

Sveiczer, A., Csikasz-Nagy, A., Gyorffy, B., Tyson, J.J., Novak, B., 2000. Modeling the fission yeast cell cycle: quantized cycle times in wee1-cdc25 mutant cells. Proc. Natl. Acad. Sci. USA 97 (14), 7865–7870.

Thomas, R., 1973. Boolean formalization of genetic control circuits. J. Theor. Biol. 42, 563–585.

Thomas, R., Thieffry, D., Kaufmann, M., 1995. Dynamical behaviour of biological regulatory networks. Biological role of feedback loops and practical use of the concept of the loop-characteristic state. Bull. Math. Biol. 57 (2), 247–276.

Thum, K.E., Shasha, D.E., Lejay, L.V., Coruzzi, G.M., 2003. Light- and carbon-signaling pathways. Modeling circuits of interactions. Plant Physiol. 132, 440–452.

Tyson, J.J., Chen, K.C., Novak, B., 2001. Network dynamics and cell physiology. Nature Rev. Mol. Cell Biol. 2, 908–916.

Tyson, J.J., Csikasz-Nagy, A., Novak, B., 2002. The dynamics of the cell-cycle regulation. BioEssays 24, 1095–1109.

Tyson, J.J., Chen, K.C., Novak, B., 2003. Sniffers, buzzers, toggles and blinkers: dynamics of regulatory and signaling pathways in the cell. Curr. Opinion Cell Biol. 15, 221–231.